Multi-Level Subcarrier Index-Power Modulated Optical OFDM with Adaptive Bit Loading for IMDD PON Systems

Al Halabi, Fadi; Chen, Lin; Giddings, Roger; Tang, Jianming; Hamie, Ali

IEEE Photonics Journal

DOI:
10.1109/JPHOT.2016.2627624

Published: 11/11/2016

Publisher's PDF, also known as Version of record

Multi-Level Subcarrier Index-Power Modulated Optical OFDM with Adaptive Bit Loading for IMDD PON Systems

F. Halabi, [1] L. Chen, [1, 2] R. P. Giddings, [1] A. Hamié, [3] and J. M. Tang [1]

[1]School of Electronic Engineering, Bangor University, LL57 1UT Bangor, U.K.
[2]College of Electronics and Information Engineering, Shanghai University of Electric Power, Shanghai 200090, China.
[3]CRITC Lab, Arts, Sciences and Technology University in Lebanon University, Beirut 1102 2801, Lebanon.

Abstract: In a previously published transmission technique known as subcarrier index-power modulated optical OFDM (SIPM-OOFDM), a new subcarrier index-power (SIP) information-bearing dimension is introduced to enable SIPM-OOFDM to carry one extra information bit per subcarrier. As a significantly improved variant of SIPM-OOFDM, in this paper, a novel signal transmission technique termed multi-level subcarrier index-power modulated OOFDM (ML-SIPM-OOFDM) is proposed and extensively explored, for the first time, which utilises four predefined subcarrier power levels to convey two extra information bits per subcarrier in the SIP information-bearing dimension. Extensive explorations of ML-SIPM-OOFDM transmission performance characteristics are undertaken, based on which optimum key transceiver parameters are identified. For cost-sensitive intensity-modulation and direct-detection (IMDD) passive optical network (PON) systems, it is shown that, compared to SIPM-OOFDM, ML-SIPM-OOFDM improves the signal transmission bit rate by 30%. In addition, in comparison with conventional OOFDM, a 13% increase in ML-SIPM-OOFDM signal transmission bit rate is also feasible without degrading the minimum received optical power required for achieving a BER of 1.0×10^{-3}. Moreover, further 9% and 10% ML-SIPM-OOFDM signal transmission bit rate enhancements are also achievable when use is made of adaptive bit loading and subcarrier count doubling, respectively.

Index Terms: Orthogonal frequency division multiplexing (OFDM), signal modulation and passive optical network (PON).

1. Introduction

The continuous growth of data network traffic associated with a large number of emerging bandwidth-hungry Internet applications and services is the fundamental driving force for the proposition of advanced high-speed and spectrally efficient transmission techniques. Recent years have seen great efforts made to improve both signal transmission bit rate and spectral efficiency by extensively exploiting numerous signal multiplexing schemes [1-4], high-order signal modulation formats [5] and appropriate combinations of both [6]. Sophisticated signal multiplexing schemes such as polarization division multiplexing (PDM) [1],[2], mode division multiplexing (MDM) [3] and space division multiplexing (SDM) [4] often require expensive optical components and/or highly complex transceiver architectures. On the other hand, the utilisation of high-order signal modulation formats escalates the demand for signal-to-noise ratio (SNR), thus leading to a rapidly increasing transceiver cost. As such, neither sophisticated signal multiplexing schemes nor high-order signal modulation formats alone are preferable for cost-sensitive passive optical networks (PONs) of interest in the present paper. For PON application scenarios, apart from the achievement of broad transmission bandwidth and high spectral efficiency in a cost-effective manner, the delivery of network operation-related features should also be addressed, which include, for example, adaptability, flexibility, backward compatibility, elasticity and power consumption efficiency.

Over the past decade, digital signal processing (DSP)-rich orthogonal frequency division multiplexing (OFDM) has gained overwhelming R&D interest worldwide because of its unique signal transmission and networking features including, for example, automatic awareness of channel spectral characteristics, excellent performance adaptability to component/system/network imperfections, high spectral efficiency, dynamically variable signal transmission bit rate versus reach performance, and DSP-enabled transceiver networking functionalities of on-line channel multiplexing/demultiplexing in the digital domain [6]. As a direct result, a number of OFDM variants have emerged for various application scenarios [7],[8]. One important variant is subcarrier index modulated OFDM (SIM-OFDM) [9]-[11] where subcarrier index is utilized as an extra information-bearing dimension to carry user information, i.e., a subcarrier is activated or deactivated according to an incoming data sequence, thus the resulting on-and-off subcarrier pattern within an OFDM symbol also bears user information. Compared to conventional OFDM, SIM-OFDM considerably improves the system bit error rate (BER) performance due to

subcarrier power reallocation, i.e., the power originally allocated to inactive subcarriers is equally redistributed amongst active ones. Therefore the power allocated to each active subcarrier is increased, thus resulting in the improved BER performance. However, in comparison with conventional OFDM, for a specific signal modulation format adopted, SIM-OFDM almost halves the achievable signal transmission bit rate and spectral efficiency, since nearly half of the subcarriers are deactivated. In addition, SIM-OFDM also suffers from the strong error propagation effect caused by the wrong detection of subcarrier power levels at the receiver.

As an attempt to address the aforementioned technical challenges associated with SIM-OFDM, very recently, subcarrier index-power modulated optical OFDM (SIPM-OOFDM) [12] has been proposed for use in cost-sensitive PON systems based on intensity-modulation and direct-detection (IMDD). In SIPM-OOFDM, the combined subcarrier index and subcarrier power acts as an extra information-carrying dimension, here referred to as subcarrier index-power (SIP) information-bearing dimension, with each subcarrier set at a low or high power according to an incoming data sequence. The resulting high and low subcarrier power pattern within an OFDM symbol enables not only all the subcarriers to be activated all the time, but also one extra information bit per subcarrier to be conveyed in the SIP information-bearing dimension. Therefore, compared to SIM-OFDM, SIPM-OOFDM significantly enhances both spectral efficiency and signal transmission bit rate without compromising the minimum SNR of the SIPM-OOFDM signal required for achieving a specific BER. More recently, SIPM-OOFDM with superposition multiplexing (SIPM-OOFDM-SPM) [13] has also been proposed and investigated, in which superposition multiplexing passively adds different signal modulation format-encoded complex numbers and assigns the sum to a high power subcarrier. Compared to SIPM-OOFDM, SIPM-OOFDM-SPM enables more effective usage of all high power subcarriers. On the other hand, both SIPM-OOFDM and SIPM-OOFDM-SPM are also capable of significantly reducing the error propagation effect [12,13]. Here it should also be pointed out, in particular, that SIPM-OOFDM and SIPM-OOFDM-SPM utilise just two subcarrier power levels to carry only one extra information bit per subcarrier in the SIP information-bearing dimension.

In this paper, we propose, for the first time, a significantly improved variant of both SIPM-OOFDM and SIPM-OOFDM-SPM, termed multi-level subcarrier index-power modulated OOFDM (ML-SIPM-OOFDM), in which four subcarrier power levels are employed to enable each subcarrier to carry two extra information bits in the SIP information-bearing dimension. Similar to SIPM-OOFDM and SIPM-OOFDM-SPM, all subcarriers are still active, each of which within a symbol is set at one of the four predefined power levels according to an incoming data sequence. Following that, the corresponding subcarrier is encoded using one of the following four signal modulation formats: binary phase shift keying (BPSK), quadrature phase shift keying (QPSK), 8-phase shift keying (8-PSK) and 16-phase shift keying (16-PSK). Generally speaking, a high (low) signal modulation format is taken on a high (low) power subcarrier. To further improve the signal transmission bit rate and system adaptability, adaptive bit loading (ABL) [14] is also applicable in ML-SIPM-OOFDM. Furthermore, in comparison with SIPM-OOFDM-SPM, ML-SIPM-OOFDM also reduces the data de-mapping function complexity in the receiver and still maintains the highly efficient usage of high power subcarriers.

For typical IMDD PON systems, it is shown that ML-SIPM-OOFDM enables a 30% improvement in signal transmission bit rate compared to QPSK/8-PSK-encoded SIPM-OOFDM. In addition, in comparison with 16-PSK-encoded conventional OOFDM, ML-SIPM-OOFDM enhances the signal transmission bit rate by 13% without degrading the minimum received optical power required at a BER of 1.0×10^{-3}. Moreover, further 9% and 10% ML-SIPM-OOFDM transmission bit rate enhancements are also feasible when use is made of ABL and subcarrier count doubling, respectively. Finally, ML-SIPM-OOFDM also has a unique feature, i.e., subcarrier count-dependent signal transmission bit rate.

TABLE 1
ML-SIPM-OOFDM Encoding Process

SIP Dimension PRBS Stream	***Subcarrier Power Level***	***Modulation Format****
0 0	First P_1	BPSK
0 1	Second P_2	QPSK
1 0	Third P_3	8-PSK
1 1	Fourth P_4	16-PSK

*without adaptive bit loading

2. ML-SIPM-OOFDM Operating Principle

The ML-SIPM-OOFDM operating principle is similar to the previously reported SIPM-OOFDM technique [12], except that the DSP functions for data encoding (decoding) in the ML-SIPM-OOFDM transmitter (receiver) are

considerably modified as detailed below. In addition, to distinguish the received power level of each individual subcarrier in the ML-SIPM-OOFDM receiver, training sequence-based new DSP functions are also developed to detect the subcarrier power status and subsequently calculate three corresponding subcarrier power thresholds for each subcarrier.

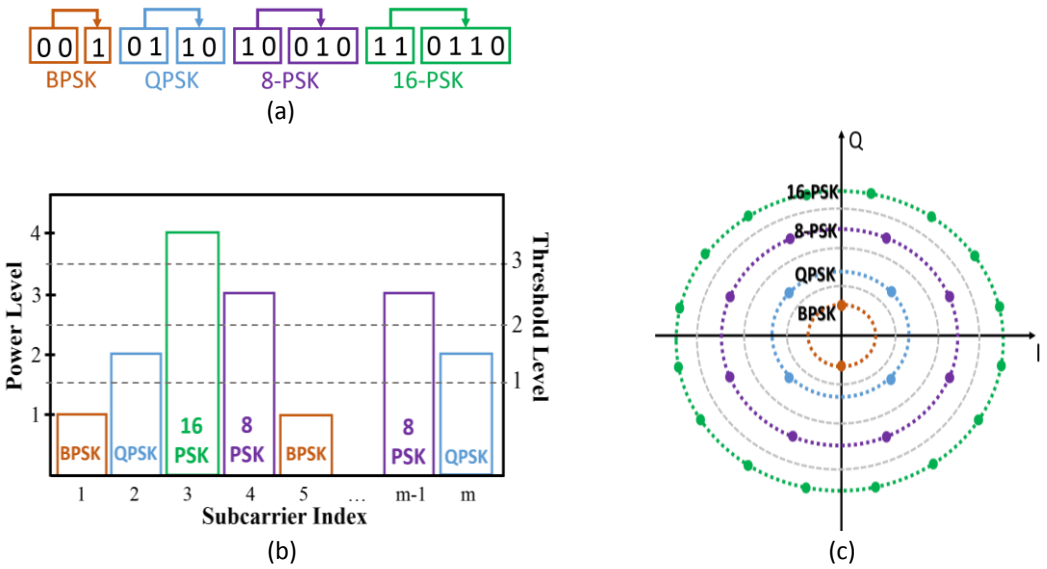

Fig. 1. (a) ML-SIPM-OOFDM data-encoding process in the transmitter. (b) Schematic diagram showing how a subcarrier of different power levels in the transmitter is encoded using BPSK, QPSK, 8-PSK, or 16-PSK. Three subcarrier power thresholds are also represented using lines that lie between each two distinct subcarrier power levels. (c) Overall ML-SIPM-OOFDM constellation.

In the ML-SIPM-OOFDM transmitter, the four subcarrier power levels are referred to as P_1, P_2, P_3 and P_4 to represent the first, second, third and fourth subcarrier power level, respectively. For simplicity, these subcarrier power levels are assumed to satisfy $P_{j+1}>P_j$ with j=1,2,3. To encode an incoming pseudo-random binary sequence (PRBS) stream, when ''00 (01)'' bits are encountered, the corresponding subcarrier power is set at P_1 (P_2), and the following 1(2) bits of the PRBS stream are truncated and subsequently encoded using BPSK (QPSK), as presented in Table 1. The resulting BPSK (QPSK)-encoded complex number is finally assigned to the subcarrier. On the other hand, when ''10 (11)'' bits are encountered in the PRBS stream, the corresponding subcarrier power is set at P_3 (P_4), and the following 3(4) bits of the PRBS stream are truncated and subsequently encoded using 8-PSK (16-PSK). The resulting 8-PSK (16-PSK)-encoded complex number is assigned to the subcarrier. Such data-encoding procedures ensure that all the information-bearing subcarriers are always active, and more importantly, each information-bearing subcarrier is capable of carrying not only two extra bits per subcarrier in the SIP information-bearing dimension but also relevant information bit(s) in the conventional subcarrier-information-bearing dimension. Examples concerning the above-described encoding procedures are illustrated in Fig. 1(a) and Fig. 1(b), and the overall ML-SIPM-OOFDM constellation is also presented in Fig. 1(c). Here it is worth mentioning the following two aspects: i) A specific subcarrier contained in an individual ML-SIPM-OOFDM symbol is encoded by randomly utilising one of these four signal modulation formats. For a long PRBS stream, the probability of encoding a specific signal modulation format on any subcarrier is 0.25. This implies that the occurrence probability of a particular constellation point presented in Fig.1(c) is different for different signal modulation format. This is verified in Fig.7; ii) apart from the 30 constellation points, each of these four subcarrier power levels in Fig.1(c) can also be regarded as “a constellation point”, as it is capable of carrying two extra information bits in the SIP information-bearing dimension.

In the ML-SIPM-OOFDM receiver, to distinguish the received power level of each individual subcarrier, DSP functions for performing both subcarrier power level detection and subcarrier threshold calculation are implemented by making use of a training sequence that is periodically inserted into the PRBS stream in the transmitter. These DSP functions are located between the fast Fourier transform (FFT) and channel estimation/equalization. For a specific subcarrier, its j-th subcarrier power threshold, $P_{T\text{-}j}$, is calculated using the formula expressed below

$$P_{T\_j} = \frac{P_{j+1} + P_j}{2} \quad j = 1,2,3 \tag{1}$$

For each subcarrier of the same frequency, $P_{T\text{-}j}$ is averaged over time to reduce the channel noise effect. These three subcarrier power thresholds are utilized to recover the extra information bits conveyed in the SIP information-bearing dimension. Furthermore, these subcarrier power thresholds are also employed to determine the signal modulation format taken on the subcarrier in the conventional subcarrier information-bearing dimension, as shown in Table I. Prior to decoding and recovering the information bits conveyed by the subcarrier in the conventional subcarrier-information-bearing dimension, channel estimation and equalization [15] are also performed using the same received training sequence. As a direct result of the system frequency response roll-off effect associated with typical IMDD PON systems, both P_j and $P_{T\text{-}j}$ are subcarrier index-dependent.

From the above-described ML-SIPM-OOFDM operating principle, it is easy to understand that the maximum ML-SIPM-OOFDM transmission bit rate is subcarrier count-dependent, this is in sharp contrast to conventional OOFDM. For an IMDD transmission system, the ML-SIPM-OOFDM transmission bit rate, R_b, can be mathematically expressed as:

$$R_b = \frac{f_s \sum_{i=1}^{N/2-1} (2 + b_i)}{N(1+\alpha)} \tag{2}$$

where f_s is the sampling rate of the digital-to-analogue converter (DAC)/analogue-to-digital converter (ADC), b_i represents the number of bits conveyed by the i-th subcarrier in the conventional subcarrier information-bearing dimension, 2 reflects the extra 2 information bits carried by the subcarrier in the SIP information-bearing dimension, N is the total number of subcarriers per symbol, and α is the coefficient introduced to take into account the signal transmission bit rate reduction due to cyclic prefix and training sequence.

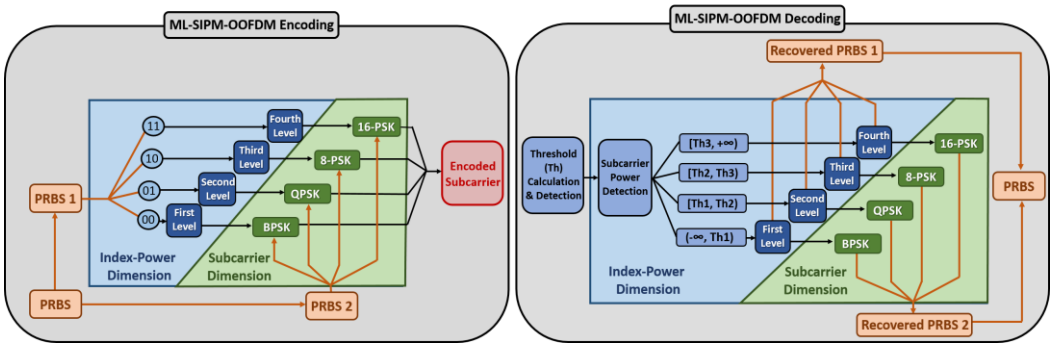

Fig.2. ML-SIPM-OOFDM signal encoding and decoding processes and major DSP functions incorporated in the receiver.

To summarize the above-descried ML-SIPM-OOFDM operating principle, Fig.2 is presented, where the signal encoding and decoding processes in both the SIP information-bearing dimension and the conventional subcarrier information-bearing dimension are illustrated using two decision-tree-like diagrams. In addition, major DSP functions incorporated in the receiver are also included in the same figure.

To effectively combat the IMDD-induced channel fading effect in a cost-effective manner, ABL widely adopted in conventional OOFDM [15,16] is also applicable in ML-SIPM-OOFDM IMDD PON systems. To apply ABL in ML-SIPM-OOFDM, the subcarrier power level to be selected still depends on the incoming data sequence, and the aforementioned data coding and decoding procedures in the SIP information-bearing dimension remain unchanged. Whilst in the conventional subcarrier information-bearing dimension, use can be made of an approach almost identical to conventional OOFDM [15,16], i.e., according to transmission channel spectral characteristics, negotiations between the transmitter and the receiver are undertaken to determine the highest signal modulation format that can be taken on each subcarrier in order to maximize the signal transmission bit rate at an overall channel BER of 1.0×10^{-3}. As a direct result, each subcarrier at a specific power level no longer corresponds to only a single fixed modulation format specified in Table I, instead, for a subcarrier at a specific power level, the corresponding signal modulation format may vary from BPSK, QPSK, 8-PSK, to 16-PSK, depending upon the channel spectral characteristics. Here, an important exception worth mentioning is that, for the vast majority of cases, high-order signal modulation formats such as 8-PSK and 16-PSK cannot be taken on subcarriers having the first and second power levels, since these relatively low subcarrier power levels considerably reduce the minimum Euclidean distances of these signal modulation formats.

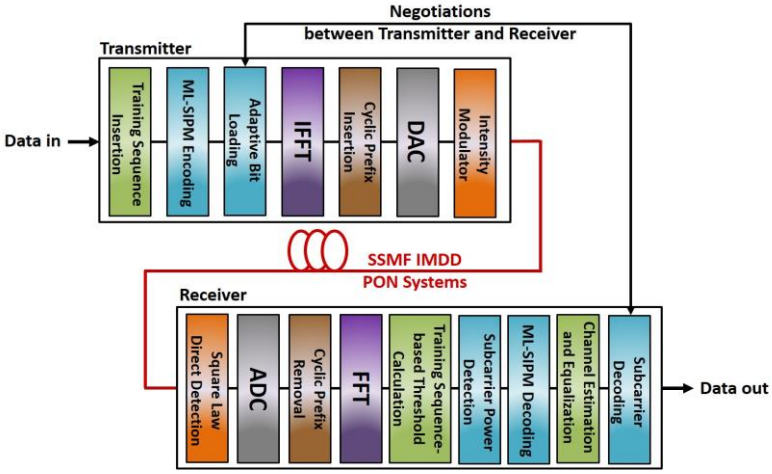

Fig. 3. Schematic illustrations of the ML-SIPM-OOFDM transceiver architecture and the considered IMDD PON transmission system.

TABLE 2
ML-SIPM-OOFDM Transceiver and IMDD PON System Parameters

Parameter	*Value*
Total number of IFFT/FFT points	64
Data-carrying subcarriers	31
Modulation formats	BPSK, QPSK, 8-PSK, 16-PSK
PRBS data sequence length	400,000 bits
Cyclic prefix	25%
DAC & ADC sample rate	12.5 GS/s
DAC & ADC bit resolution	9 bits
Clipping ratio	12 dB
PIN detector sensitivity	-19dBm*
PIN responsivity	0.8 A/W
SSMF dispersion parameter at 1550 nm	16 ps/(nm.km)
SSMF dispersion slope at 1550 nm	0.07 ps/nm/nm/km
Linear fiber attenuation	0.2 dB/km
Kerr coefficient	2.35×10^{-20} m²/W

*Corresponding to 10 Gb/s non-return-to-zero data at a BER of 1.0×10^{-9}

3. Optimisations of Key Transceiver Parameters

3.1. ML-SIPM-OOFDM Transceiver Architecture and IMDD PON System

The ML-SIPM-OOFDM transceiver architecture and the IMDD PON transmission system considered in this paper are illustrated in Fig. 3. As seen in this figure, the ML-SIPM-OOFDM transmitter consists of several DSP functions that are identical to those employed in SIPM-OOFDM [12], SIPM-OOFDM-SPM [13] and conventional OOFDM [14,15,16]. These identical DSP functions include, for example, PRBS stream generation, training sequence insertion, as well as the arrangement of all encoded information-bearing subcarriers to satisfy the Hermitian symmetry with respect to their conjugate counterparts to ensure the generation of real-valued OFDM symbols after performing the inverse FFT (IFFT). In particular, new DSP functions are also included to perform the ML-SIPM-OOFDM data-encoding operations described in Section 2. In addition, for a specific transmission system, an ABL DSP function is also implemented to ensure the adaptation of highest possible signal modulation formats on any subcarriers in the conventional subcarrier information-carrying dimension. At the output of the IFFT, cyclic prefix addition and digital-to-analogue conversion are undertaken to produce a final electrical signal, which is then utilised to drive an optical intensity modulator to perform the electrical-to-optical (E-O)

conversion. To explicitly highlight the salient performance features of the proposed technique, throughout this paper, an ideal optical intensity modulator is considered, which produces an optical output signal, $s_o(t)$, having an amplitude waveform governed by

$$s_o(t) = \sqrt{s_e(t)} \quad (3)$$

where $s_e(t)>0$ is the electrical driving current of the ML-SIPM-OOFDM signal with a corresponding optimum DC bias current being added.

A standard single-mode fibre (SSMF) simulation model based on the widely adopted split-step Fourier method is adopted to model the propagation of optical signals over the IMDD PON systems [17]. In the SSMF simulation model, the effects of linear loss, chromatic dispersion and Kerr effect-induced dependence of the refractive index upon optical power are also included [17].

After fibre transmissions, the optical signal is converted to the electrical domain by a square-law photodetector subject to both shot and thermal noise. These two noise effects are simulated following the procedures similar to those presented in [17]. As illustrated in Fig.3, the major receiver DSP functions include: detection of the training sequence, cyclic prefix removal, FFT for generating complex-valued frequency domain subcarriers utilizing received real-valued time domain symbols, subcarrier power detection, subcarrier power threshold calculation, recovery of information bits conveyed in the SIP information-bearing dimension, channel estimation and equalization, recovery of data carried in the conventional subcarrier information-bearing dimension, as well as analysis of individual subcarrier BERs and overall channel BERs.

To numerically simulate the ML-SIPM-OOFDM transmission performance over the IMDD PON system of interest in the present paper, the adopted key transceiver and system parameters are listed in Table 2. Unless stated explicitly in the corresponding text, these parameters are utilised as default throughout this paper. Our numerical simulation results also show that ML-SIPM-OOFDM and SIPM-OOFDM have almost same peak-to-average power ratios (PAPRs). As a direct result, an optimum clipping ratio of 12dB (listed in Table 2) is identical to that optimised in the SIPM-OOFDM transceivers [12].

3.2. Optimizations of Subcarrier Power Levels

Due to the fact that each information-bearing subcarrier contains one of the four predefined different power levels, it is therefore envisaged that the adaptation of optimum subcarrier power levels plays a vital role in determining the maximum achievable ML-SIPM-OOFDM transmission performance. As such in this section special attention is first given to optimizing these subcarrier power levels. It is easy to understand that the received absolute optimum subcarrier power at the j-th level, P_j, varies with subcarrier index because of the channel fading effect. To take into account such an effect, in the following optimisation process, instead of employing an absolute subcarrier power level, use is made of a subcarrier power level ratio, PR_j, defined as

$$PR_j = \frac{P_j}{P_1} \quad \text{j=2,3,4} \quad (4)$$

For simplicity, in the transmitter P_1 =1 is assumed regardless of subcarrier index. Such treatment is valid because channel equalization in the receiver is always conducted on subcarrier basis. In addition, for simplicity without loss of generality, in the optimisation process, additive white Gaussian noise (AWGN) channels are also considered and ABL is excluded.

The adopted numerical optimization procedures are outlined as follows:

1. A subcarrier power level ratio parameter set, $\{b_U\} = \{PR_2, PR_3, PR_4\} = \{3, 5, 7\}$, is adopted as the initial input parameter values.
2. Numerical simulations are undertaken with the first element, PR_2, varying within a reasonable range, and all other parameters fixed at their original values. An optimum PR_2 is obtained when a minimum overall channel BER is reached.
3. Numerical simulations are then performed by simultaneously considering the following two conditions: a) the next element in $\{b_U\}$ is selected to vary within a reasonable range, and b) all the previously adopted elements in $\{b_U\}$ remain unchanged except that the elements optimised in this iteration are fixed at their optimum values. An optimum value of the selected element is obtained when a minimum overall channel BER is reached.
4. Step 3 repeats until all the elements contained in $\{b_U\}$ are optimised.
5. By making use of the newly generated parameter set $\{b_U\}$, Step 2, Step 3 and Step 4 are repeated to produce a further updated version of $\{b_U\}$. Such iterative procedure continues until <2% variations of all the elements in $\{b_U\}$ are reached with respect to their corresponding values obtained in last iteration.

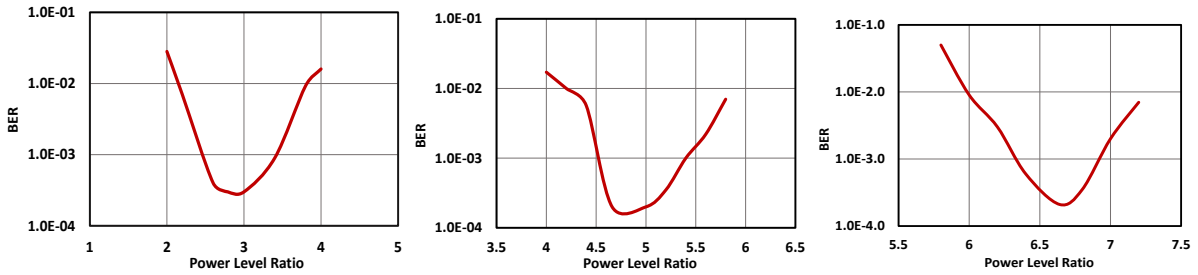

Fig. 4. Overall channel BER as a function of subcarrier power level ratio. (a) Overall BER versus PR_2 with PR_3 and PR_4 fixed at their optimum values; (b) Overall BER versus PR_3 with PR_2 and PR_4 fixed at their optimum values; (c) Overall BER versus PR_4 with PR_2 and PR_3 fixed at their optimum values. Here AWGN channels with input ML-SIPM-OOFDM signal SNRs fixed at 18dB are considered in all simulations.

Based on the above-mentioned optimisation procedure, after just 3 iterations, the final optimum subcarrier power level ratios are identified, which are $PR_2 = 2.79$, $PR_3 = 4.66$ and $PR_4 = 6.64$. Furthermore, by making use of Eq.(1) and $P_1 = 1$, the three optimum subcarrier power thresholds can also be deduced easily, which are $P_{T-1} = 1.90$, $P_{T-2} = 3.73$, and $P_{T-3} = 5.65$. These six optimum parameters are taken as default values throughout the paper.

To explicitly demonstrate how the overall channel BER performance varies as a function of individual subcarrier power level ratio, Fig. 4 is plotted, where the electrical AWGN channels are considered and the input ML-SIPM-OOFDM signal SNRs are fixed at 18dB. In obtaining each of these three figures, except for the variable subcarrier power level ratio, all other two remaining subcarrier power level ratios are fixed at their optimum values. It is shown in Fig. 4 that for all the cases considered, the overall channel BERs grow with increasing offsets from their optimum values. The occurrence of these optimum subcarrier power level ratios is mainly due to the combined effects of the following three physical mechanisms:

- A variation in the power difference between two adjacent subcarrier power levels alters the accuracy in detecting the received subcarrier power status. This directly affects the BERs corresponding to both the SIP information-bearing dimension and the conventional subcarrier information-bearing dimension via error propagation.
- A variation in the subcarrier power level alters the minimum Euclidean distance of the corresponding signal modulation format taken on the subcarrier. This directly affects BERs because of errors occurring in the conventional subcarrier information-bearing dimension.
- A change to one subcarrier power level causes relevant alterations to all other subcarrier power levels across all subcarriers, as the total ML-SIPM-OOFDM signal power always remains constant.

By making use of the abovementioned physical mechanisms, it is very easy to understand the occurrence of optimum subcarrier power level ratios in both Fig.4(a) and Fig.4(b). In Fig.4(c), for subcarrier power level ratios lower than 6.64, the BER grows with decreasing subcarrier power level ratio, this mainly results from the fast reduction in the minimum Euclidean distance of the 16-PSK constellation. Whilst for subcarrier power level ratios larger than 6.64, the observed BER increase with increasing subcarrier power level ratio occurs because of the fixed electrical signal power-induced reductions in minimum Euclidean distance for the BPSK, QPSK and 8-PSK constellations.

4. ML-SIPM-OOFDM Transmission Performance

After having completed the optimisations of key transceiver parameters in Section 3, the thrust of this section is to explore the maximum achievable ML-SIPM-OOFDM transmission performance over various transmission systems. In addition, the impacts of subcarrier count and ABL are also investigated on the achievable ML-SIPM-OOFDM transmission bit rate versus reach performances.

By making use of the transceiver parameters listed in Table 2 and the optimum parameters identified in Section 3, the maximum achievable signal transmission bit rates of SIPM-OOFDM, conventional OOFDM encoded with QPSK, 8-PSK and 16-PSK, as well as ML-SIPM-OOFDM can be calculated very easily, which are summarized in Table 3, where the average number of bits transmitted per subcarrier is also listed for each transmission technique considered. It can be seen in Table 3 that the proposed technique gives rise to a signal transmission bit rate of 26.80Gb/s, which significantly exceeds 16-PSK-encoded OOFDM and QPSK/8-PSK-encoded SIPM-OOFDM by approximately 13% and 30%, respectively. The fact that ML-SIPM-OOFDM has the

ability of significantly outperforming any of these previously published transmission techniques encoded using similar signal modulation formats implies that for a specific transmission system, the ML-SIPM-OOFDM-induced improvement in signal transmission bit rate does not compromise considerably the system power budget, as discussed in Section 4.1.

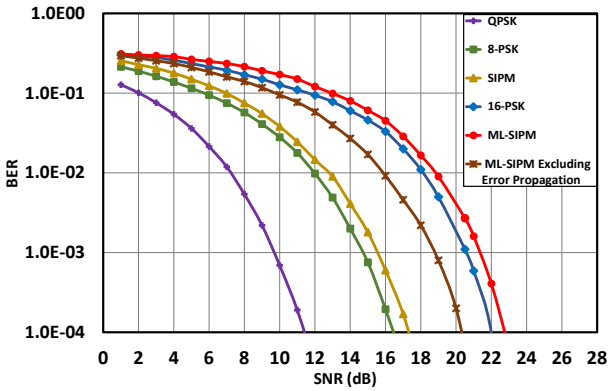

Fig. 5. Overall channel BER performance versus signal SNR over AWGN channels for ML-SIPM-OOFDM, SIPM-OOFDM and conventional OOFDM encoded using QPSK, 8-PSK and 16-PSK.

TABLE 3
Signal Transmission Bit Rate Comparisons

Modulation Format	*Signal Bit Rate (Gb/s)**	*Average Bits per Subcarrier*
QPSK	11.87	2
8-PSK	17.80	3
SIPM	20.77	3.5
16-PSK	23.73	4
ML-SIPM	26.80	4.5

*31 data-carrying subcarriers are used

4.1. ML-SIPM-OOFDM Transmission Performances over AWGN Channels and IMDD PON Systems

For achieving specific BERs, the impacts of ML-SIPM-OOFDM on minimum required electrical signal SNR over AWGN channels are presented in Fig. 5, where BER performance comparisons are made between QPSK/8-PSK-encoded SIPM-OOFDM, conventional OOFDM uniformly encoded with QPSK, 8-PSK and 16-PSK, as well as ML-SIPM-OOFDM. To clearly distinguish the influence of the error propagation effect on minimum required signal SNR at a BER of 1.0×10^{-3}, an error propagation-free ML-SIPM-OOFDM BER curve is also computed and subsequently plotted in Fig.5. Based on the approach reported in [12], in computing the error propagation-free curve, the signal modulation format taken on each individual subcarrier is first compared between the transmitter and the receiver. A signal modulation format difference indicates the occurrence of a subcarrier power detection error. When such an error occurs, the corresponding error bits conveyed in the SIP information-carrying dimension are removed, and also a corresponding number of random bits is added (removed) when a lower (higher) signal modulation format is detected in the receiver compared to the transmitter. To highlight the ML-SIPM-associated impacts, ABL is excluded for all the cases presented in Fig.5.

As expected, it is very interesting to note in Fig.5 that the 26.80Gb/s ML-SIPM-OOFDM signal has an overall BER developing trend very similar to a 23.73Gb/s 16-PSK-encoded conventional OOFDM signal, and between these two signals, there exists a SNR difference as small as 1.0dB at a BER of 1.0×10^{-3}. In addition, in the same figure, a very similar SNR difference is also observed between QPSK/8-PSK-encoded SIPM-OOFDM and 8-PSK-encoded OOFDM.

Furthermore, by comparing the ML-SIPM-OOFDM BER curves between the cases of including and excluding the error propagation effect, it is easy to find in Fig.5 that the error propagation effect introduces an approximately 2.6dB SNR penalty. More importantly, compared to conventional OOFDM encoded using 16-PSK, error propagation-free ML-SIPM-OOFDM gives rise to a SNR gain as large as 1.7dB. The physical origin of the 1.7dB SNR gain is mainly due to the fact that 16-PSK is just taken randomly on a relatively small portion of the information-carrying subcarriers in ML-SIPM-OOFDM, thus resulting in an increase in the overall minimum Euclidean distances of all signal modulation formats taken on other subcarriers because of the constant signal power employed. The above results suggest that ML-SIPM-OOFDM has great potential of not only considerably improving the signal transmission bit rate, but also significantly decreasing the minimum required signal SNR, when the present simple subcarrier power detection algorithms are modified to effectively minimise the error propagation effect.

The BER performance of 26.80Gb/s ML-SIPM-OOFDM signal transmission over 25km SSMF IMDD PON systems is presented in Fig. 6, where the BER performances are also shown for 20.77Gb/s QPSK/8-PSK-encoded SIPM-OOFDM signals, 23.73Gb/s 16-PSK OOFDM signals, 17.80Gb/s 8-PSK OOFDM signals, as well as 11.87Gb/s QPSK-OOFDM signals. In numerically simulating Fig.6, the optical launch powers are taken to be -9dBm and once again ABL is excluded. Fig. 5 shows that ML-SIPM-OOFDM has a very similar BER performance to 16-PSK OOFDM, and

between these two transmission techniques there exists a received optical power difference of approximately 0.5dB at a BER of 1.0×10^{-3}. This agrees very well with the corresponding electrical SNR difference observed in Fig.5. Such phenomenon implies that the ML-SIPM-introduced 13% increase in signal transmission bit rate just causes approximately 0.5dB changes to both the received optical power and optical power budget at a BER of 1.0×10^{-3}. In addition, our simulation results also show that compared to 16-PSK OOFDM, ML-SIPM-OOFDM does not degrade the system performance tolerances to fibre chromatic dispersion and nonlinearity. Such behaviours are very similar to those discussed in detail in [12], thus corresponding system performance tolerance results are not presented in this paper.

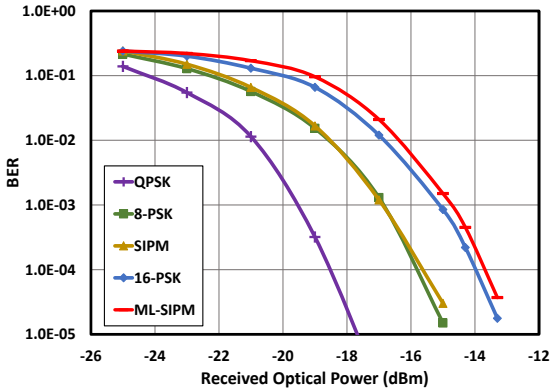

Fig. 6. Overall channel BER versus received optical power after transmitting through 25km SSMF IMDD PON systems for QPSK/8-PSK-encoded SIPM-OOFDM, ML-SIPM-OOFDM, and conventional OOFDM encoded using QPSK, 8-PSK and 16-PSK.

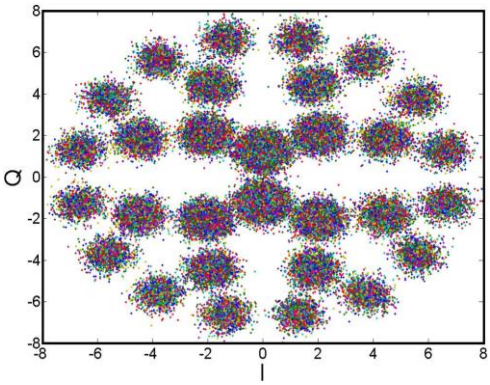

Fig. 7. ML-SIPM-OOFDM constellation after equalization at a BER of 1.0E-3 after transmission over 25km SSMF IMDD PON systems. In simulating this figure, the optical launch power is fixed at -9dBm.

The representative overall ML-SIPM-OOFDM constellation obtained after equalization at a BER of 1.0×10^{-3} is illustrated in Fig. 7, after 25km SSMF IMDD PON transmission subject to an optical launch power of -9dBm. In Fig. 7, the sizes of the constellation points associated with relatively low signal modulation formats are larger than those corresponding to relatively high signal modulation formats, this is because the occurrence probability of a specific constellation point of the low signal modulation format is higher than that corresponding to the high signal modulation format because all the signal modulation formats are encoded at an equal probability.

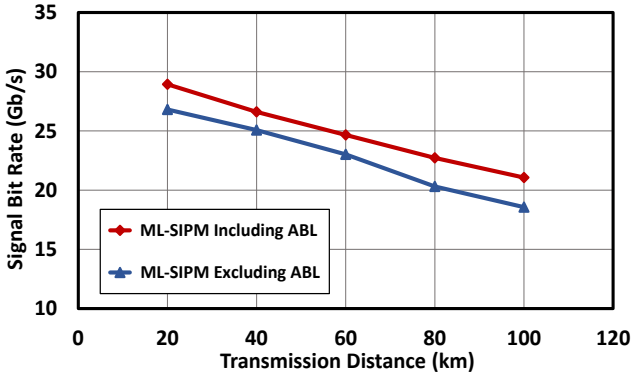

Fig. 8. Maximum achievable ML-SIPM-OOFDM transmission bit rate as a function of transmission distance over IMDD SSMF PON system. Optical launch powers are fixed at -9dBm. ABL: adaptive bit loading.

4.2. Impacts of ABL and Subcarrier Count

The effectiveness of utilising ABL in improving the ML-SIPM-OOFDM transmission data rate is explored in Fig.8, where maximum achievable ML-SIPM-OOFDM transmission bit rate versus reach performances for fixed optical launch powers of -9dBm are presented for two cases of including and excluding ABL. In implementing ABL, for a given transmission distance, negotiations between the transmitter and the receiver take place to determine the highest signal modulation format that can be taken on each individual subcarrier under the condition that the overall channel BER of $\leq 1.0\times10^{-3}$ is still satisfied. As already stated in Section 2, depending upon the channel spectral response experienced by a subcarrier, any power level of a subcarrier may be encoded using signal modulation formats varying from BPSK, to QPSK, to 8-PSK and to 16-PSK. Furthermore, for long transmission

distances, the strong channel fading effect may cause high frequency subcarriers to suffer from excessive errors even if the lowest signal modulation formats are taken on them. When such a situation occurs, those high frequency subcarriers are dropped completely.

It is shown in Fig. 8 that for IMDD PON transmission distances up to 100km, ABL is capable of improving the ML-SIPM-OOFDM transmission bit rate by approximately 9%, and such improvement is transmission distance-independent. These simulated behaviours agree extremely well with OOFDM experimental measurements reported in [18]. The agreements not only confirm the validity and accuracy of the numerical simulations presented here, but also imply the ML-SIPM-OOFDM capability of perfectly preserving the effectiveness of ABL regardless of transmission distance. On the other hand, very similar to ABL, adaptive power loading (APL) also results in almost identical signal transmission bit rate improvements for ML-SIPM-OOFDM, SIPM-OOFDM and conventional OOFDM. The impact of APL is, however, not shown in the present paper as detailed discussions has already been made in [12, 15].

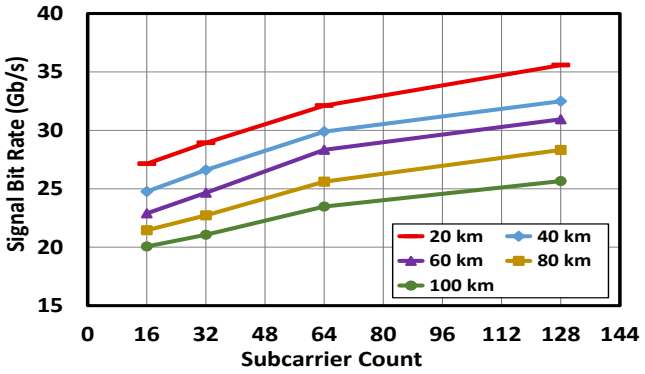

Fig. 9. Subcarrier count-dependent ML-SIPM-OOFDM transmission bit rate for different transmission distances. Optical launch powers are fixed at -9dBm. Adaptive bit loading is applied for all the cases considered.

As discussed in Section 2, the achievable ML-SIPM-OOFDM transmission bit rate is a function of subcarrier count. To gain an in-depth understanding of the subcarrier count-dependent ML-SIPM-OOFDM transmission bit rate for various transmission distances, Fig. 9 is presented, in which the optical launch powers are fixed at -9dBm and ABL is also applied for all the cases. It can be seen in Fig. 9 that an approximately 10% transmission bit rate enhancement is feasible when the subcarrier count is doubled. As an example, for any transmission distances in Fig. 9, an increase of almost 30% in ML-SIPM-OOFDM transmission bit rate is achievable when increasing the subcarrier count from 16 to 128. In addition, the large subcarrier count-induced transmission bit rate improvement is also independent of transmission distance, as the transmission bit rate curves for different transmission distances exhibit parallel developing trends, as seen in Fig. 9.

Very similar to ABL and APL, the large subcarrier count-enabled enhancement in ML-SIPM-OOFDM transmission bit rate does not comprise the system power budget. In practical transmission system design, the management of ML-SIPM-OOFDM subcarrier count may provide an effective means to dynamically and adaptively trade the achievable signal transmission bit rate with available transceiver DSP logic resources.

5. Conclusions

As a significantly improved variant of the previously proposed SIPM-OOFDM technique capable of just carrying one extra information bit per subcarrier in the newly introduced SIP information-bearing dimension, ML-SIPM-OOFDM has been proposed and numerically investigated extensively, for the first time, which simultaneously conveys four subcarrier power level-supported two extra information bits in the SIP information-bearing dimension. Extensive explorations of ML-SIPM-OOFDM performance characteristics have been undertaken, based on which optimum key transceiver parameters are identified. For cost-sensitive IMDD SSMF PON systems, it has been shown that, compared to QPSK/8-PSK-encoded SIPM-OOFDM, ML-SIPM-OOFDM improves the signal transmission bit rate by 30%. In addition, in comparison with conventional OOFDM encoded using 16-PSK, a 13% increase in ML-SIPM-OOFDM signal transmission bit rate is also feasible without degrading the minimum required received optical power at a BER of 1.0×10^{-3}. Moreover, our results have also indicated that further 9% and 10% ML-SIPM-OOFDM transmission bit rate enhancements are also achievable when use is made of ABL and subcarrier count doubling, respectively.

References

[1] M. Ye et al., ''On-chip multiplexing conversion between wavelength division multiplexing–polarization division multiplexing and wavelength division multiplexing–mode division multiplexing,'' *Opt. Lett*., vol. 39, no. 4, pp. 758-761, Feb. 2014.

[2] D. Qian, N. Cvijetic, Y. Huang, and J. Yu, "22.4-Gb/s OFDM transmission over 1000 km SSMF using polarization multiplexing with direct detection," *Optical Fiber Communication (OFC) Conference,* pp. 1-3, Mar. 2009.

[3] T. Mori, T. Sakamoto, M. Wada, T. Yamamoto, and F. Yamamoto, "Fewmode fibers supporting more than two LP modes for mode-division multiplexed transmission with MIMO DSP," *J. Lightw. Technol.*, vol. 32, no. 14, pp. 2468–2479, Jul. 2014.

[4] P. Khodashenas et al., ''Comparison of spectral and spatial super-channel allocation schemes for SDM networks,'' J. Lightw. Technol., vol. 34, no. 11, pp. 2710–2716, Jun. 2016.

[5] P. J. Winzer, ''High-spectral-efficiency optical modulation formats,'' *J. Lightw. Technol.,* vol. 30, no. 24, pp. 3824-3835, Dec. 2012.

[6] X. Duan, R.P. Giddings, M. Bolea, Y. Ling, B. Cao, S. Mansoor and J.M. Tang, "Real-time experimental demonstrations of software reconfigurable optical OFDM transceivers utilizing DSP-based digital orthogonal filters for SDN PONs" Optics Express, vol.22, no.16, pp.19674-19685, Aug. 2014.

[7] X. Ouyang et al., ''Experimental demonstration and field-trial of an improved optical fast OFDM scheme using intensity-modulation and full-field detection,'' *J. Lightw. Technol.*, vol. 33, no. 20, pp. 4353-4359, Aug. 2015.

[8] X. Chen et al., 'Hybrid modulated multiband coherent optical OFDM for low-complexity phase noise compensation,'' *J. Lightw. Technol.*, vol. 33, no. 1, pp. 126-132, Jan. 2015.

[9] M. Wen, "On the achievable rate of OFDM with index modulation," *IEEE Trans. Signal Process*., vol. 64, no. 8, pp. 1919-1932, Nov. 2015.

[10] A. Amin et al., ''Performance evaluation of coded optical subcarrier index modulation OFDM format,'' *Optical Fiber Communication (OFC) Conference*, pp. 1-3, Mar. 2013.

[11] E. Başar, Ü. Aygölü, E. Panayırcı, and H. Vincent Poor, "Orthogonal frequency division multiplexing with index modulation," *IEEE Trans.* Signal Process., vol. 61, no. 22, pp. 5536–5549, Nov. 2013.

[12] F. Halabi, L. Chen, S. Parre, S. Barthomeuf, R. P. Giddings, C. Aupetit-Berthelemot, A. Hamié, and J. M. Tang, ''Subcarrier index-power modulated optical OFDM and its performance in IMDD PON systems,'' J. Lightw. Technol., vol. 34, no. 9, pp. 2228–2234, May 2016.

[13] L. Chen, F. Halabi, R. P. Giddings and J. M. Tang, "Subcarrier index-power modulated optical OFDM with superposition multiplexing for IMDD transmission systems," J. Lightw. Technol., vol.34, Oct. 2016. (accepted for publication).

[14] E. Giacoumidis, A. Kavatzikidis, A. Tsokanos, J. M. Tang, and I. Tomkos, ''Adaptive loading algorithms for IMDD optical OFDM PON systems using directly modulated lasers,'' *Opt. Commun. Netw*., vol. 4, no. 10, pp. 769–778, Oct. 2012.

[15] R. Giddings, "Real-time digital signal processing for OFDM-base future optical access networks," *J. Lightw. Technol.*, vol. 32, no. 4, pp. 553–570, Feb. 2014.

[16] E. Giacoumidis, J.L. Wei, X. L. Yang, A. Tsokanos, and J. M. Tang, ''Adaptive-modulation-enabled WDM impairment reduction in multichannel optical OFDM transmission systems for next-generation PONs,'' *IEEE Photon. J*., vol. 2, no. 2, pp. 130-140, Apr. 2010.

[17] G. P. Agrawal, *Fibre-Optic Communication Systems,* 2nd ed. Hoboken, NJ, USA, Wiley, 1997.

[18] X. Q. Jin, J. L. Wei, R. P. Giddings, T. Quinlan, S. Walker, and J. M. Tang, ''Experimental demonstrations and extensive comparisons of end-to-end real-time optical OFDM transceivers with adaptive bit and/or power loading,'' *IEEE Photon. J.,* vol. 3, no. 3, pp. 500-511, Jun. 2011.